Garibbo, S, Blondel, P, Heald, G, Heyburn, R, Hunter, AJ & Williams, D 2022, '**Measurements of shipping, fin whales, earthquakes and other soundscape components at the Lofoten-Vesterålen Observatory, Norway (2018-2019)**',

Proceedings of Meetings on Acoustics, vol. 47, 070017. https://doi.org/10.1121/2.0001619

https://www.overleaf.com/project/62d034ca78887d01b03355d1

ABSTRACT

Underwater soundscapes are complex as they are a combination of several components with overlapping acoustic frequencies and different timescales, from individual durations to seasonality and long-term trends. Sounds below 100 Hz are of particular interest to compare human impacts (e.g. shipping and geophysical exploration) with natural processes (e.g. earthquakes and weather) and animal vocalisations (e.g. whales), but understanding is often limited to specific signals on their own, not their combination . We have processed over two years (2018 and 2019) of measurements from the Lofoten-Vesterålen cabled ocean observatory, located 15 km offshore northern Norway, at a depth of 255 m. Earlier analyses (Garibbo et al., 2020,[1] Garibbo et al., 2021[2]) identified the different contributions of weather, shipping and earthquakes in data collected in 2018, using deep learning to automatically detect common 20 Hz fin whale calls. The results of the deep learning approach are compared to a new, improved shipping detector, based on traditional spectral analyses, showing the complementarity of each approach. By extending these analyses using data from 2019, we can quantify the standard soundscape components based on origins, frequency ranges and seasonality, and assess their variability over time. Some sources (e.g. earthquakes) can be thousands of kilometres from the observatory, showing low-frequency soundscapes include information over large regions of the ocean. This paper summarises the main findings of this work including a description of the analysis methods used and the resulting components of the soundscapes. These extensive results provide a useful baseline for further studies of other low-frequency environments around the world.

INTRODUCTION

Sounds dominate the oceans, spanning all frequencies and coming from different sources: natural (e.g. wind, rain), biological (e.g. marine mammals, fish) and anthropogenic (e.g. ships, seismic exploration). Very-low frequency hydroacoustic signals ($<$ 100 Hz) are often associated with geophysical processes, like earthquakes and landslides, but they can also be linked to man-made activities, like offshore industry, fish blasting, or even nuclear test explosions. Understanding the mechanisms generating noise below 100 Hz, has important applications for monitoring nuclear explosions (for example, the combined use of seismic, hydroacoustic and infrasound signals to detect and study distant phenomena, particularly explosions, but also submarine accidents or aircraft impacts), and to naval operations such as anti-submarine warfare, where noise can be either or both a source of interference and a source of opportunity. Current understanding of these mechanisms is very limited for noise below 100 Hz and the ocean acoustic phenomena below 10 Hz are rarely studied and even less well understood. Very often, the strong background noise will include several distinct sources, some of which can be very close and others louder but propagating from very large ranges, up to ocean-scale. It is therefore very important to understand the key acoustic signatures of these processes, along with their extreme spatial and temporal variability. The measuring and resolving power of ocean observatories can be harnessed to investigate low-frequency ambient noise over long timescales, and in a variety of background noise conditions.

DATA AND METHOD

The data presented here are taken from the Lofoten-Vesterålen (LoVe) observatory (Fig. 1), which is located approximately 15 km offshore of the Lofoten Islands, at a depth of 255 m on the continental shelf.[3] It is situated within the Hola Trough - one of many troughs formed during the last glaciation - and hosts cold water coral reefs, sandwave fields, and glacigenic deposits.[4–6] The hydrophone (a calibrated Ocean Sonic

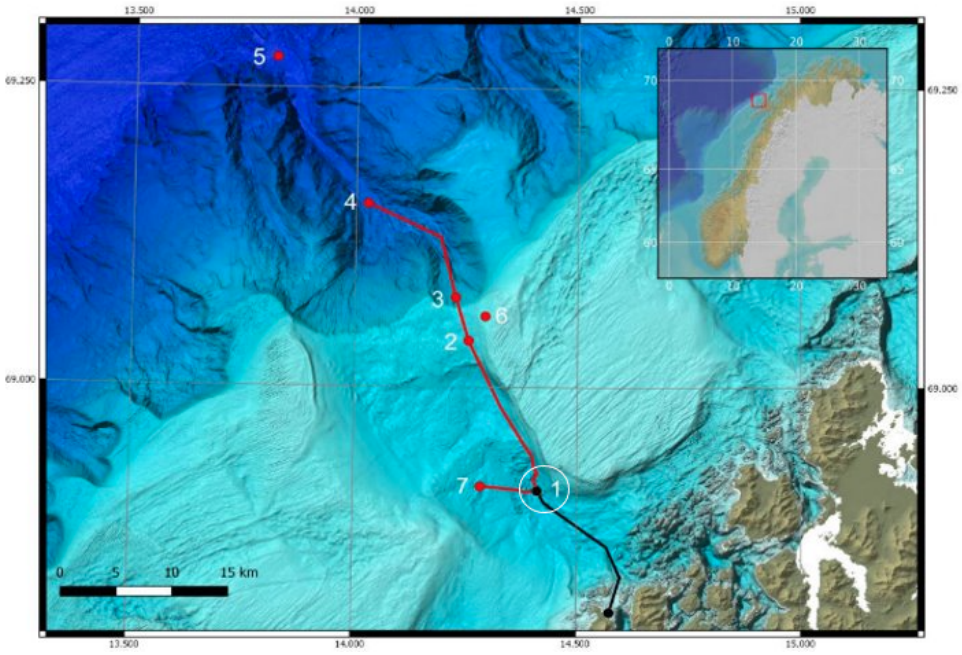

Figure 1: Layout of LoVe observatory offshore of the Lofoten Islands (insert shows the location offshore northern Norway marked with a red box); numbers 1 to 7 are used to label hydrophone nodes.[3] The location of the hydrophone is at node 1.

SB35 ETH) records between 10 Hz and 200 kHz, and is mounted approximately 0.5 m above the seabed on a metallic structure which is anchored into the seabed.[7]

The data was initially processed using Matlab software called PAMGuide, which performs calibrated signal processing on passive acoustic data in both terrestrial and aquatic environments.[8] The calibration parameters were taken from the Ocean Sonic hydrophone specifications,[7] and compared to previous work done at LoVe.[3] However, as the analysis progressed, it became apparent that automatic signal processing techniques would be necessary due to the large volume of different signals of interest. Three different approaches to signal identification are outlined here.

A. A DEEP LEARNING DETECTOR FOR 20 HZ FIN WHALE CALLS

The most commonly found whale vocalisation in the LoVe dataset is attributed to the fin whale, and is known as the "20 Hz call".[9,10] An example of this call is shown in Fig. 4. The global distribution of fin whales mean that this high amplitude, and long-distance propagating call is a common feature of the world's ocean soundscape.[11] It is thought to be a call made by male fin whales during breeding season to attract females from great distances[11,12] as unlike other whales, fin whales do not gather in specific areas to mate.[13] The high call density called for the use of a form of automatic detection.

Deep learning 'learns' data characteristics through multiple layers of processing - layers closest to the input data extract simple features, and the layers closest to the output data extract more complex features from the lower layers.[14] The 'learning' done in deep learning refers to weights and biases between layers, which are fine-tuned on each iteration of a deep learning algorithm to exhibit a desired behaviour - in the case of image classification, this behaviour would be correctly classifying an image,[15] a task which has achieved human-level accuracy in the last decade.[16,17]

Using Ketos - a Python software package which was developed in 2019 by Meridian, which provides a user-friendly interface for acoustic researchers with minimal knowledge of deep learning[18] - 2863 examples

of 20 Hz fin whale calls (of SNR ranging from 20 to 113) in the LoVe data were used to train a residual neural network. A full explanation of this process can be found in Garibbo *et al.* 2021.[2] The deep learning detector ultimately reached a performance of 93.7% accuracy, a precision of 99.4%, and a recall rate of 94.2% (where accuracy is true positive - the definitions for which can be seen below.

$$Accuracy = \frac{TP+TN}{TP+FP+TN+FN} \quad Precicion = \frac{TP}{TP+FP} \quad Recall = \frac{TP}{TP+FN}$$

Where TP is true positive detection, TN is true negative, FP is false positive, and FN is false negative.

B. A TONAL SHIPPING DETECTOR

Identifying and quantifying all shipping noise present in the LoVe data without access to data on local ships' Automatic Identification Systems (AIS) proved a challenge. Ultimately a simple tonal peak detector was constructed in Matlab (version R2021a) to run over the first and second frequency bands outlined in the European Marine Strategic Framework Directive (MSFD)[19] for monitoring noise pollution attributed to shipping. After pre-processing in PAMGuide (described previously),[8] the Power Spectral Density (PSD) in each 1 Hz interval of each audio file was bandpass filtered for each MSFD band. The data were then split into 60 second windows and the 10^{th}, 50^{th}, and 90^{th} percentiles were calculated across each window. Matlab's in-built "findpeaks"[20] function was then used to locate peaks in each percentile that exceeded a minimum prominence threshold - a value which was determined by manual spectral analysis of a randomly-sampled selection of data where shipping noise was present and where it was not. Every peak detected in each percentile was then recorded. The detector performance is outlined in Fig.2. The vast majority of instances where shipping was incorrectly classified as ambient noise consisted of non-tonal shipping noise, or tonal shipping noise undergoing Doppler shift or a Lloyds Mirror-type effect.

	Annotated Shipping	Annotated Ambient Noise
Shipping detection	369	40
Noise detection	57	178

Figure 2: Performance of the tonal shipping detector - accuracy of 84.9%, precision of 90.2%, recall of 86.6% - definitions for which are displayed above.

C. EARTHQUAKE IDENTIFICATION

An arbitrary area was selected around LoVe to simultaneously constrain the number of earthquakes that would be present in a two year period to a number manageable for manual analysis, and also possibly contain a variety of potential geophysical acoustic sources - for example, glaciers in Greenland and Svalbard, the Mid-Atlantic Ridge, and volcanic activity in Iceland. The open-access International Seismological Centre (ISC)[21] bulletin was used to identify all earthquakes that occurred within this arbitrary area over the two year time period. An earthquake was considered detected if the signal appeared in the LoVe data within one second of the predicted travel time. The predicted travel times were generated through an open-source software TauP,[22] where the required input parameters for the calculation included the geodesic distance between the earthquake epicentre and the LoVe hydrophone, and the source depth. For many earthquakes in the ISC bulletin, source depths are either fixed or are poorly constrained. Although errors in the source

depth will affect the predicted arrival times at LoVe, the well-know trade-off between earthquake origin time and source depth means that these errors are compensated for in the origin time. The predicted travel times were computed from the IASP91 velocity model option available within TauP,[22] as this a standard model for calculating travel times of the main seismic phases through the solid earth.[23]

Another type of arrival to consider with earthquakes is known as the T phase - a type of wave that has travelled both through the Earth as a seismic phase, and in the water column as an acoustic wave. The challenge with T phase travel time prediction is that the point of conversion from seismic phase to acoustic phase is usually unknown. Therefore, the criteria chosen for the picking of possible T phases were: 1) that the duration of the signal is greater than 5 seconds, 2) that the signal does not exhibit the characteristic appearance of the seismic arrivals in spectrogram format - see Fig.3 for elaboration, and 3) that the signal arrives later than corresponding predicted seismic arrival times.

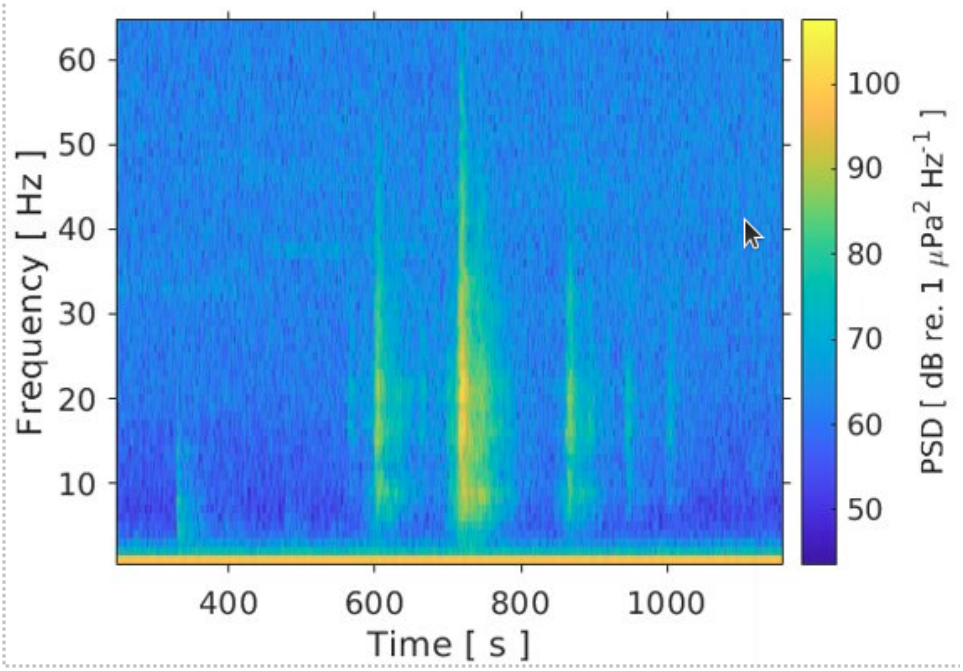

Figure 3: On the left of the spectrogram (before 400 s), a seismic P phase is seen. Seismic phases are generally concentrated in intensity around frequencies < 20 Hz for 1 second or less. Suspected T phases are shown at 600 s to the end of the spectrogram. These tend to consist of higher intensity signals over a larger frequency range. Note: the loss in signal intensity of the suspected T phases at 10 Hz and below are likely related to a roll-off (from 10 Hz to 0 Hz) high pass filter applied by the hydrophone manufacturer.[7]

RESULTS

20 HZ FIN WHALE VOCALISATIONS

The number of 20 Hz fin whale calls peaks across both years in January, February, March, and December, as seen in Fig. 4. This coincides with the fin whale breeding season in the northern hemisphere,[24] when the 20 Hz calls are expected to peak in frequency. There is a notable drop in call detections from the 10^{th} to 30^{th} January, and a rapid drop between February and the beginning of March, where detections increase again towards the end of the month.

There are instances where a drop in call detection - such as in January 2018 - coincides with a period of increased shipping, and a dominant wind in a northeasterly direction,[25] which would blow over the Love

hydrophone in the absence of a shielding landmass - see Fig. 1. An explanation could be that the 20 Hz calls present were masked by environmental noise (e.g. wind, local shipping noise) - a possibility that is supported by the lower SNRs of the misclassified noise. However, it may be that the fin whales stopped vocalising or changed song type,[26] or passed into a region that was not conducive to sound propagating to LoVe, as the location of the source whales is unknown.

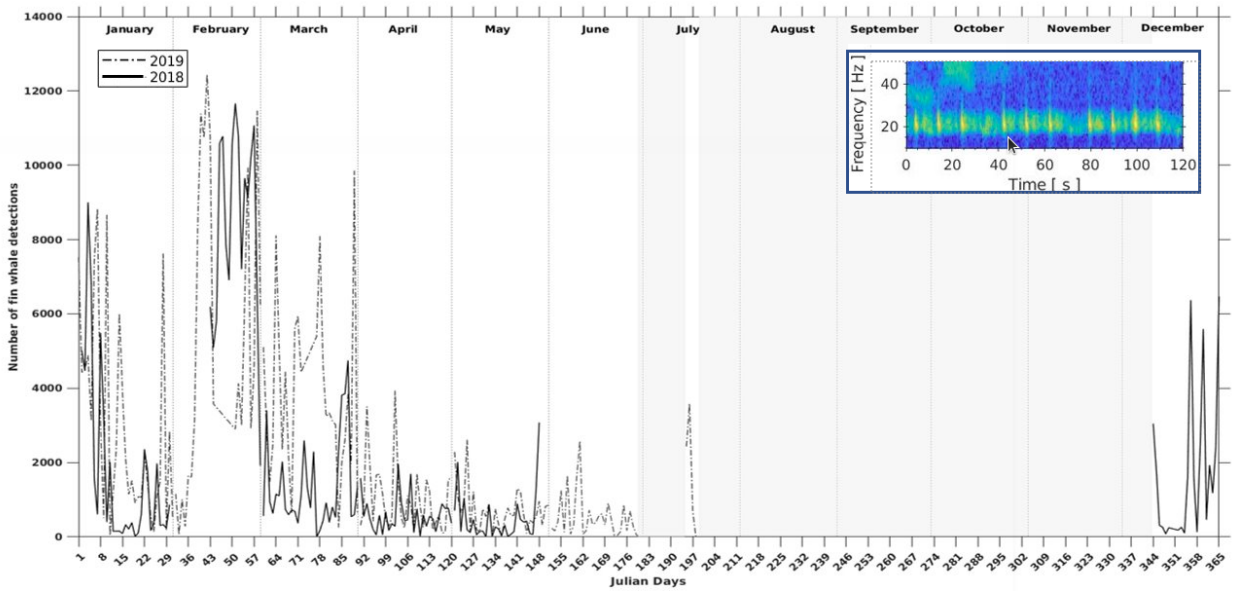

Figure 4: Ketos detections from all available data in 2018 (solid black line) and 2019 (dashed black line). The grey boxed areas show periods of time with no available or usable data. The blue insert shows an example spectrogram of the 20 Hz fin whale calls that are used in Ketos for analysis.

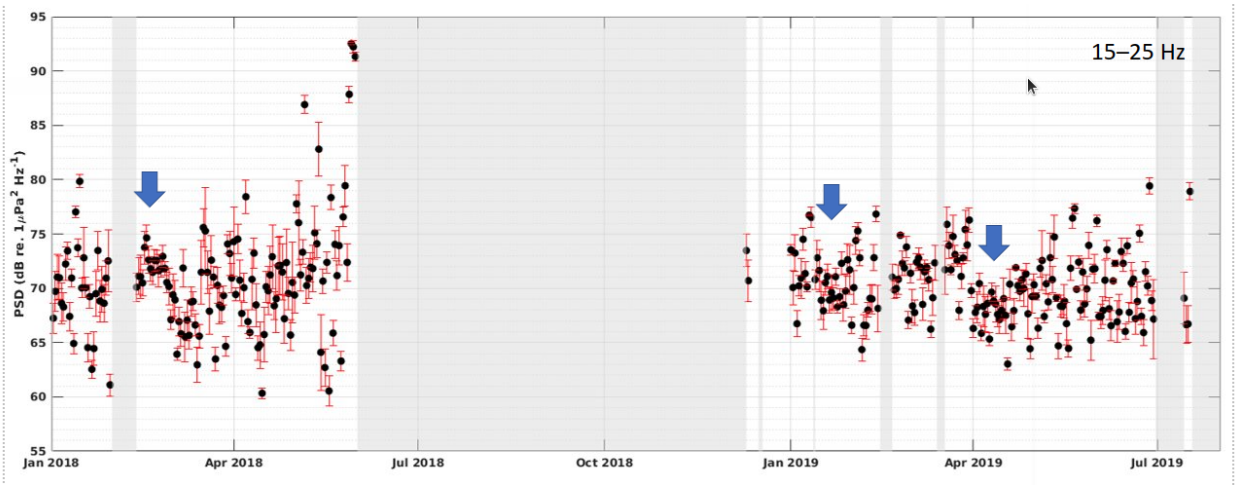

Figure 5: Calibrated PSD values between 15 Hz and 25 Hz for Ketos detections from all available data in 2018 and 2019 . The grey boxed areas show periods of time with no available or use-able data. The blue arrows highlight periods where the standard deviation of the detected 20 Hz calls slightly decreases and the average PSD of the calls fluctuate less. It is possible that this may reflect periods of time where the whales are geographically constrained.

The PSD levels of the received 20 Hz calls are displayed in Fig. 5. The PSD levels of the calls vary considerably from month to month, with the most well-constrained PSD measurements occurring in February. The variation in PSD likely reflects the source whales' average distance from the hydrophone, but it may also be that the extent to which the measurements are constrained is dictated by how geographically constrained the source whales are.

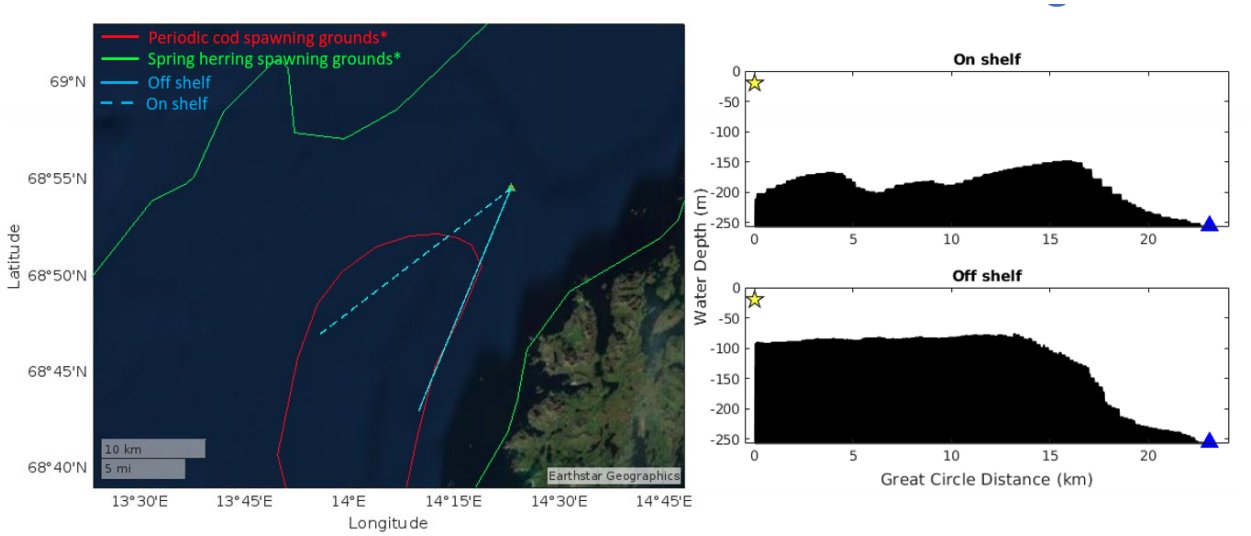

Figure 6: LHS: a map showing the LoVe hydrophone (triangle) in relation to nearby known areas of fish spawning (data from Mareano[27]), which could serve as possible nearby feeding grounds for fin whales.[28] RHS: example of bathymetry track between the LoVe hydrophone and an arbitrary on-shelf point selected within the nearby cod spawning ground (solid cyan line on map), and example of an arbitrary off-shelf point (dashed cyan line). These examples highlight the complexity of the bathymetry in the local area.

A reasonable cause for the fin whales being geographically constrained would be an abundance of food in a particular location.[28] Fig. 6 displays the most proximal fish stock spawning grounds to the LoVe hydrophone. Determining what locations are most likely to be where some of the loudest fin whale calls in the data are coming from requires propagational modelling, which forms a part of ongoing and future work.

SHIPPING

Tonal shipping noise was observed in almost every day of data - as can be seen in Fig. 7. We know from other work done around LoVe that the majority of shipping noise heard at the observatory during 2018 is from ships that are over 5 km away - and mostly between 20 km and 25 km away during the winter months.[29] We see more shipping noise in MSFD band 2 than we do in MSFD band 1, but the PSD level of the shipping noise across each band is generally higher in band 1 - see Fig. 7.

EARTHQUAKES

Hydrophones commonly detect seismic phases and T phases from earthquakes,[30–32] and in total, 143 earthquakes were found in the LoVe data in 2018, and 290 earthquakes were found in 2019 - as can be seen in Fig. 8. As shown on the maps, the majority of detected earthquakes (in light green) are along the segment of the Mid-Atlantic Ridge (MAR) that is closest to the hydrophone - particularly on a ridge segment that is known as Mohns Ridge. Mohns Ridge is a slow-spreading segment of the MAR and the most southern

portion of it exhibits continuous ridge-focused volcanic activity[33,34] - which coressponds to the location of most of the epicentres of the earthquakes detected at LoVe.

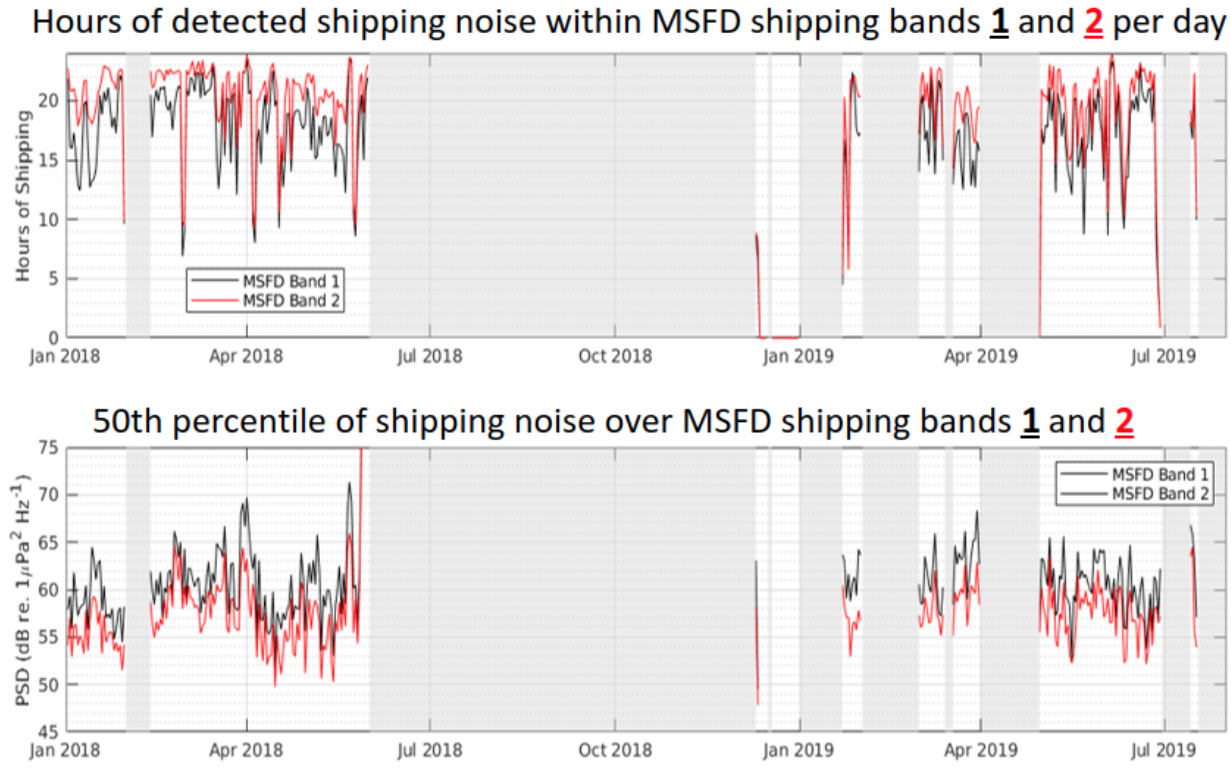

***Figure 7:** Top: Hours of shipping noise detected in the LoVe data over 2018 and 2019 across MSFD band 1 (black) and MSFD band 2 (red). Bottom: PSD of detected shipping noise over 2018 and 2019. Band 1 refers to the 63 Hz third octave level, and band 2 the 125 Hz third octave level.*

Possible reasons that some earthquakes were detected whilst others, especially if from similar locations were not, could involve different earthquake magnitudes, different paths of propagation, and the sound levels at LoVe. The acoustic and seismic signals of earthquakes of a magnitude of 2 or less are unlikely to propagate as far as a larger magnitude earthquake,[32] and the propagation paths from some geological regions may mean that a signal is far less likely to reach LoVe. For example, the region of the Mid-Atlantic Ridge to the south of Iceland appears to be a location from which an earthquake signal rarely appears at LoVe. As can be seen in the bathymetry of Fig. 8, this coincides with two large fracture zones - the Charlie-Gibbs and the Bight Fracture Zones. Fractured rock results in delays in the seismic arrival times, and reduces the signal amplitude,[35] which may contribute to the number of events going undetected at LoVe. Other possible explanations for undetected events could involve the bathymetry between the epicentre and LoVe - for example, in Fig. 8 a bathymetric high (the Rockall Rise) is visible to the northwest of the U.K., and presents a possible barrier to acoustic signals from events originating south of Iceland - but to determine this, thorough testing of propagation models would be necessary. Other explanations for undetected earthquakes at LoVe also include a rise in local ambient noise, as a result of a storm for instance, or that the arrival coincides with a masking transient noise at LoVe like shipping.

CONCLUSION

Between 2018 and 2019 in we have observed seasonal variation in the occurrence of the 20 Hz fin whale call and periods of well-constrained PSD that could possibly reflect periods where the fin whales are geographically constrained. We have identified possible source locations for the loudest measured calls, and their feasibility can be assessed through propagational modelling.

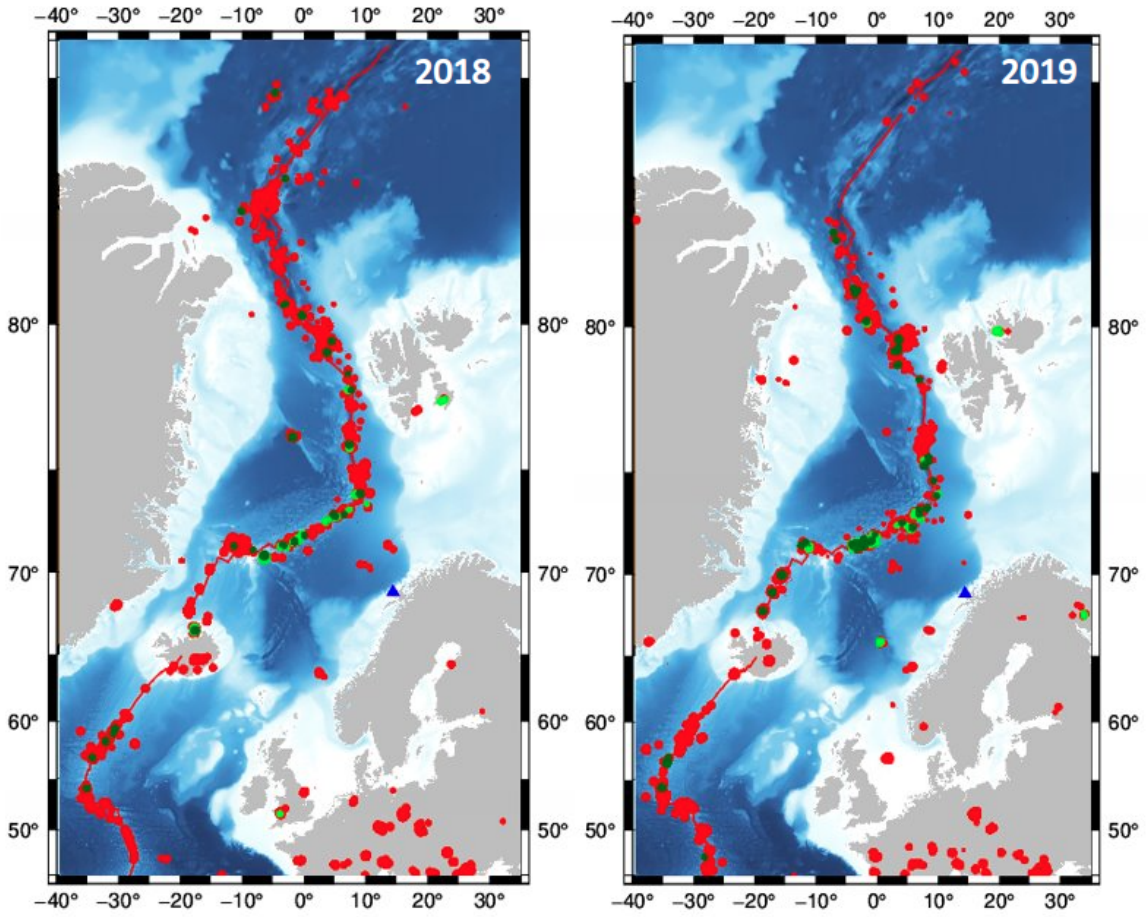

Figure 8: Earthquakes from the ISC in marked as circles, and the LoVe hydrophone marked as a blue triangle. Red circles are earthquakes that were not detected at LoVe (blue triangle), light green circles are earthquakes that were detected by their seismic phases, and dark green are earthquakes that were possibly detected by T phase as well - verification of this would require propoagational modelling. The earthquake marker sizes reflect the earthquake magnitude. The red line represents the Mid-Atlantic Ridge, and the bathymetry data is from GEBCO[36]

More shipping noise is observed in the second MSFD band that the first, but the PSD is higher in the first MSFD band. When plotted on the Wenz curve[37] - see Fig. 9, we can see that the sound levels of the shipping noise in the first MSFD band agree with the upper limit for shipping in shallow water.

The majority of earthquakes that are detected at the LoVe observatory originate from Mohns Ridge - the closest section of the MAR. Most of the arrivals from earthquakes are seismic phases, but a few possible T phases have been identified using the criteria previously mentioned, and validation of these phases would require propagational modelling.

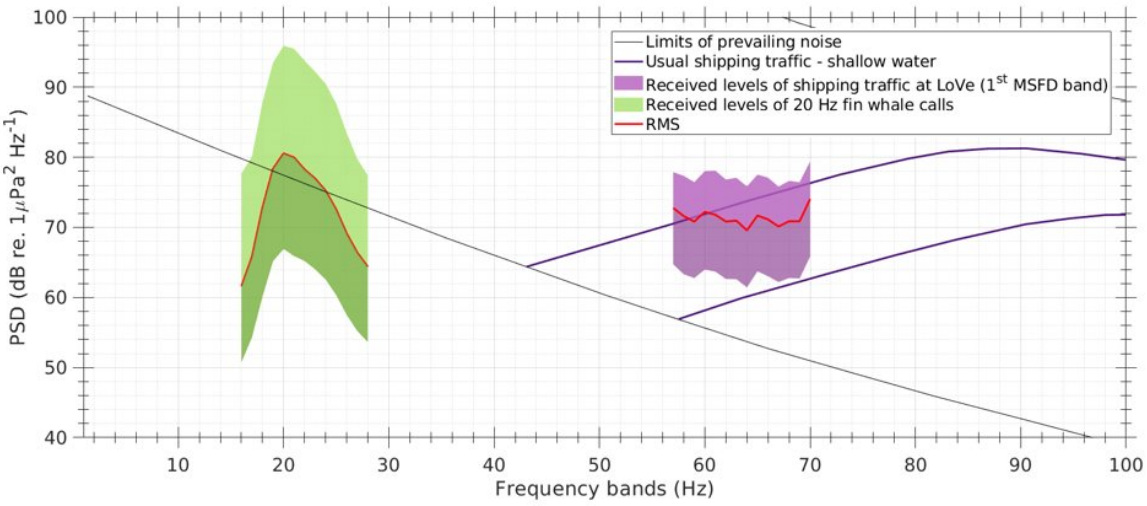

Figure 9: A Wenz curve[37] of the LoVe data from 2018 to 2019: shipping noise from the first MSFD band is in shaded purple, and the green shaded area represents the 20 Hz fin whale calls - the upper and lower limits of the shaded areas represent the 90^{th} and 10^{th} percentiles of noise respectively. The earthquakes cannot be fairly represented in this plot due to the lower sensitivity limit of the hydrophone.

ACKNOWLEDGEMENTS

This research is supported by the UK Engineering and Physical Sciences Research Council (EPSRC), as part of industrial Cooperative Award in Science and Technology (iCASE) project #2279119, supported by Defence Science & Technology Laboratory (Dstl) and AWE Forensic Seismology. Crown Copyright (2022) © Dstl, AWE.

REFERENCES

[1] S. Garibbo, Ph. Blondel, G. Heald, R. Heyburn, A. Hunter, D. Williams, "Low-frequency ocean acoustics – measurements from the Lofoten-Vesterålen Ocean Observatory, Norway", *Proceedings of meetings on acoustics Acoustical Society of America*, **40:1**, 040001 (2020).

[2] S. Garibbo, Ph. Blondel, G. Heald, R. Heyburn, A. Hunter, D. Williams, "Characterising and detecting fin whale calls using deep learning at the Lofoten-Vesterålen Observatory, Norway", *Proceedings of meetings on acoustics Acoustical Society of America*, **44**, 070021 (2021).

[3] L. Ødegaard, G. Pedersen, E. Johnsen, "Underwater Noise from Wind at the High North LoVe Ocean Observatory", *UACE 2019 Conference Proceedings*, 359–366 (2019).

[4] S. Sauer, A. Crémière, J. Knies, A. Lepland, D. Sahy, T. Martma, S. R. Noble, J. Schönenberger, M. Klug, C.J. Schubert, "U-Th chronology and formation controls of methane-derived authigenic carbonates from the Hola trough seep area, northern Norway", *Chemical Geology* **470**, 164–179 (2017).

[5] T. Van England, O. R. Godø, E. Johnsen, G. C. A. Duineveld, D. van Oevelen, "Cabled ocean observatory data reveal food supply mechanisms to a cold-water coral reef",*Progress in Oceanography*, **172**, 51–64 (2019).

[6] R. Bøe, V. K. Bellec, M. F. J. Dolan, P. Buhl-Mortensen, L. Buhl-Mortensen, D. Slagstad, L. Rise, "Giant sandwaves in the Hola glacial trough off Vesterålen, North Norway", *Marine Geology* **267:1**, 36–54 (2009).

[7] Metas, "Ocean Observatory Vesterålen", Statoil, URL: https://love.statoil.com/Resources/LoVe%20Ocean%20Observatory%20Sensor%20System.pdf (2014)

[8] N. D. Merchant, K. M. Fristrup, M. P. Johnson, P. L. Tyack, M. J. Witt, P. Blondel, S. E. Parks, "Measuring Acoustic Habitats", *Methods in Ecology and Evolution*, **2041-210X.12330** (2015).

[9] A. Pereira, D. Harris, P. Tyack, L. Matias, "Lloyd's mirror effect in fin whale calls and its use to infer the depth of vocalizing animals", *Proceedings of Meetings on Acoustics*, **27**, 070002, (2016).

[10] S. J. Buchan, L. Gutierrez, N. Balcazar-Cabrera, K. M. Stafford, "Seasonal occurrence of fin whale song off Juan Fernandez, Chile", *Endangered Species Research*, **39:1998**, 135–145 (2019).

[11] J. L. Morano, D. P. Salisbury, A. N. Rice, K. L. Conklin, K. L. Falk, C. W. Clark, "Seasonal and geographical patterns of fin whale song in the western North Atlantic Ocean", *The Journal of the Acoustical Society of America*, **132:2**, 1207–1212 (2012).

[12] M. G. Aulich, R. D. McCauley, D. Robert, B.J. Saunders, M.J.G. Parsons, "Fin whale (Balaenoptera physalus) migration in Australian waters using passive acoustic monitoring", *Nature Scientific Reports*, **9**, 1–12 (2019).

[13] D. A. Croll, C. W. Clark, A. Acevedo, B. Tershy, S. Flores, J. Gedamke, J. Urban, "Only male fin whales sing loud songs", *Nature*, **417:6891**, 809–809 (2002).

[14] P. P. Shinde, S. Shah, "A Review of Machine Learning and Deep Learning Applications", *Proceedings - 2018 4th International Conference on Computing, Communication Control and Automation 2018*, *ISBN: 9781538652572* (2018).

[15] J. Schmidhuber, "Deep learning in neural networks: An overview", *Neural Networks*, **61**, 85–117 (2015).

[16] O. S. Kirsebom, F. Fabio, Y. Simard, N. Roy, S. Matwin, S. Giard, "Performance of a deep neural network at detecting north atlantic right whale upcalls", *The Journal of the Acoustical Society of America*, **147**, 2637–2646 (2020).

[17] K. He, X. Zhang, S. Ren, J. Sun, "Delving Deep into Rectifiers: Surpassing Human-Level Performance on ImageNet Classification", *arXiv:1502.01852*, (2015).

[18] Meridian, "Welcome to Ketos's documentation!", https://docs.meridian.cs.dal.ca/ketos/: *Accessed on 07/05/2021*, (2020)

[19] European Commission, "Directive 2008/56/EC of the European Parliament and of the Council of 17 June 2008, establishing a framework for community action in the field of marine environmental policy (Marine Strategy Framework Directive)", *Official Journal of the European Union*, **L164**, 19–40 (2008).

[20] Matlab, "findpeaks", *Matlab Documentation [Online]*, https://uk.mathworks.com/help/signal/ref/findpeaks.html, **Date accessed: 12/07/22**, (2007–2016).

[21] International Seismological Centre, Online Bulletin, https://doi.org/10.31905/D808B830 (2020).

[22] H. P. Crotwell, T. J. Owens, J. Ritsema, "The TauP Toolkit: Flexible seismic travel-time and ray-path utilities", *Seismological Research Letters*, **70**, 154-160 (1999).

[23] B.L.N. Kennett, E.R. Engdahl, "Travel times for global earthquake location and phase association.", *Geophysical Journal International*, **105**, 429–465 (1991).

[24] S. L. Nieukirk, K. M. Stafford, D. K. Mellinger, R. P. Dziak, and C. G. Fox, "Low-frequency whale and seismic arigum sounds recorded in the mid-Atlantic Ocean", *The Journal of the Acoustical Society of America*, **115:4**, 1832–1843 (2004).

[25] H. Hersbach, B. Bell, P. Berrisford, S. Hirahara, A. Horányi, J. Muñoz-Sabater, J. Nicolas, JC. Peubey, R. Radu, D. Schepers, A. Simmons, C. Soci, S. Abdalla, X. Abellan, G. Balsamo, P. Bechtold, G. Biavati, J. Bidlot, M. Bonavita, G. De Chiara, P. Dahlgren, D. Dee, M. Diamantakis, R. Dragani, J. Flemming, R. Forbes, M. Fuentes, A. Geer,L. Haimberger, S. Healy, R. J. Hogan, E. Hólm, M. Janisková, S. Keeley, P. Laloyaux, P. Lopez, C. Lupu, G. Radnoti, P. de Rosnay, I. Rozum, F. Vamborg, S. Villaume, J. N. Thépaut. "The ERA5 global reanalysis", *Quarterly Journal of the Royal Meteorological Society*, **146:730**, 1999–2049 (2020).

[26] B. Hendricks, E. M. Keen, C. Shine, J. L. Wray, H. M. Alidina, C. R. Picard, "Acoustic tracking of fin whales: Habitat use and movement patterns within a Canadian Pacific fjord system", *The Journal of the Acoustical Society of America*, **149:6**, 4264-4280 (2021).

[27] Mareano, "The Sea in Maps and Pictures [Online]", https://mareano.no/en (2022).

[28] Garcia, H. A., Zhu, C., Schinault, M. E., Kaplan, A. I., Handegard, N. O., Godø, O. R., Ahonen, H., Makris, N. C., Wang, D., Huang, W., Ratilal, P., "Temporal-spatial, spectral, and source level distributions of fin whale vocalizations in the Norwegian Sea observed with a coherent hydrophone array.", textslICES Journal of Marine Science, **76:1**, 268-–283 (2019).

[29] A. S. Aniceto, E. L. Ferguson, G. Pedersen, A. Tarroux, R. Primicerio, "Temporal patterns in the soundscape of a Norwegian gateway to the Arctic", *Nature Scientific Reports*, **12**, 7655 (2022).

[30] D. K. Blackman, C. E. Nishimura, J. A. Orcutt, "Seismoacoustic recordings of a spreading episode on the Mohns Ridge", *Journal of Geophysical Research: Solid Earth*, **105:B5**, 10961–10973 (2000).

[31] R. P. Dziak, D. R. Bohnenstiehl, H. Matsumoto, C. G. Fox, D. K. Smith, M. Tolstoy, T. K. Lau, J. H. Haxel, M. J. Fowler, "P- and T-wave detection thresholds, Pn velocity estimate, and detection of lower mantle and core P-waves on ocean sound-channel hydrophones at the Mid-Atlantic Ridge", *Bulletin of the Seismological Society of America*, **94:2**, 665–677 (2004).

[32] P. D. Slack, C. G. Fox, R. P. Dziak, "P wave detection thresholds, Pn velocity estimates, and T wave location uncertainty from oceanic hydrophones", *Journal of Geophysical Research: Solid Earth*, **104:B6**, 13061–13072 (1999).

[33] A. Lim, M. Brönner, S. E. Johansen, M. Dumais, "Hydrothermal Activity at the Ultraslow-Spreading Mohns Ridge: New Insights From Near-Seafloor Magnetics", *Geochemistry, Geophysics, Geosystems*, **20:12**, 5691–5709 (2019).

[34] L. J. Elkins, K. W. W. Sims, J. Prytulak, J. Bilchert-Toft, T. Elliott, J. Blusztajn, S. Fretzdorff, M. Reagan, K. Haase, S. Humphris, J. G. Schilling, "Melt generation beneath Arctic Ridges: Implications from U decay series disequilibria in the Mohns, Knipovich, and Gakkel Ridges", *Geochimica et Cosmochimica Acta*, **127**, 140–170 (2014).

[35] F. K. Boadu, L. T. Long, "Effects of fractures on seismic-wave velocity and attenuation", *Geophysical Journal International*, **12:1**, 86-110 (1996).

[36] GEBCO Compilation Group (2020) GEBCO 2020 Grid (doi:10.5285/a29c5465-b138-234d-e053-6c86abc040b9)

[37] G. M. Wenz, "Acoustic ambient noise in the ocean: spectra and sources", *The Journal of the Acoustical Society of America*, **34:12**, 1936–1956 (1962).